HHS Public Access

Author manuscript

Epilepsia. Author manuscript; available in PMC 2020 June 01.

Published in final edited form as:

Epilepsia. 2019 June ; 60(6): 1255–1265. doi:10.1111/epi.15969.

Hypervascularization in mTOR-dependent focal and global cortical malformations displays differential rapamycin-sensitivity

Longbo Zhang[1,2], **Tianxiang Huang**[1,2], **Shannon Teaw**[2], and **Angélique Bordey**[2,*]

[1]Department of Neurosurgery, Xiangya Hospital, Central South University, 85 Xiangya Street, Changsha, 410008, China

[2]Departments of Neurosurgery and Cellular & Molecular Physiology, Yale University School of Medicine, New Haven, CT 06520-8082

Summary

Objectives—Patients with mTOR-dependent malformations of cortical development (MCDs) associated with seizures display hyperperfusion and increased vessel density of the dysmorphic cortical tissue. Some studies suggested that the vascular defect occurred independently of seizures. Here, we further examined whether hypervascularization occurs in animal models of global and focal MCD with and without seizures, and whether it is sensitive to the mTOR blocker, rapamycin, that is approved for epilepsy treatment in tuberous sclerosis complex.

Methods—We used two experimental models of mTOR-dependent MCD consisting of conditional transgenic mice containing *Tsc1*^{null} cells in the forebrain generating a global malformation associated with seizures and wildtype mice containing a focal malformation in the somatosensory cortex generated by in utero electroporation (IUE) that does not lead to seizures. Alterations in blood vessels and the effects of a two-week long rapamycin treatment on these phenotypes were assessed in juvenile mice.

Results—Blood vessels in both the focal and global MCDs of postnatal day 14 mice displayed significant increase in vessel density, branching index, total vessel length, and decreased tissue lacunarity. In addition, rapamycin treatment (0.5 mg/kg, every two days) partially rescued vessel abnormalities in the focal MCD model, but it did not ameliorate the vessel abnormalities in the global MCD model that required higher rapamycin dosage for a partial rescue.

Significance—Here, we identified hypervascularization in mTOR-dependent MCD in the absence of seizures in young mice, suggesting that increased angiogenesis occurs during development in parallel to alterations in corticogenesis. In addition, a predictive functional outcome is that dysplastic neurons forming MCD will have better access to oxygen and metabolic supplies via their closer proximity to blood vessels. Finally, the difference in rapamycin sensitivity

*Correspondence to: Angélique Bordey, Ph.D., Department of Neurosurgery, Yale University School of Medicine, 333 Cedar Street, FMB 422, New Haven, CT 06520-8082, Phone: 203-737-2515, Fax:203-737-2159, angelique.bordey@yale.edu.

Disclosure: None of the authors has any conflict of interest to disclose. We confirm that we have read the Journal's position on issues involved in ethical publication and affirm that this report is consistent with those guidelines.

Ethical Publication Statement: We confirm that we have read the Journal's position on issues involved in ethical publication and affirm that this report is consistent with those guidelines.

between a focal and global MCD suggest that rapamycin treatment will need to be titrated to match the type of MCD.

Keywords

tuberous sclerosis complex; focal cortical dysplasia; hyperperfusion; mTOR; rapamycin; everolimus; epilepsy; tuber; vessel; microvessel; hypervascularization

Introduction

Malformations of cortical development (MCDs) are often (80-90%) associated with epilepsy and developmental delay in young children and are among the most common causes of intractable epilepsy[1-3]. A large subset of MCDs result from de novo somatic mutations occurring during brain development affecting mTOR pathway genes[4-13] and share similar cytoarchitectural abnormalities. Those include: 1) Focal cortical dysplasia type II (FCDII) and tuberous sclerosis complex (TSC) characterized by disruption of normal cortical laminar structure within a restricted (or focal) cortical region and the presence of large dysmorphic neurons; and 2) hemimegalencephaly characterized by hemispheric loss of laminar structure and the presence of dysmorphic neurons[14-16].

In epilepsies due to MCDs and hippocampal sclerosis, ictal activity is accompanied with hyperperfusion of the epileptogenic foci[17-21]. Hyperperfusion, which corresponds to increased blood flow, has been commonly associated with elevated metabolic needs of neurons in the epileptic foci[22]. However, recent evidence also suggests that hyperperfusion may be related to vessel alterations, and in particular increased vessel density, that were reported in MCDs from patients with hemimegalencephaly and FCD[18; 19] Such vascular alteration is conceivable considering that mTOR hyperactivity in TSC and FCDII-related MCD in mice and humans leads to increased production of vascular endothelial growth factor (VEGF) that regulates angiogenesis[23-26]. Nevertheless, experimental data related to vessel alterations in mTOR-dependent MCD are limited. Another unaddressed question is whether the vasculature alterations are rapamycin-sensitive and thus mTOR-dependent. This is an important question because an analog of rapamycin, which blocks mTOR activity, has been approved for epilepsy treatment in TSC patients and decreased seizure frequency in 40% of the patients at the highest dose tested[27].

Here, we thus set out to investigate whether vessel density was altered in experimental models of mTOR-dependent MCD in mice. The models consisted of wildtype mice containing a mTOR-dependent focal malformation in the somatosensory cortex that does not lead to seizures[28] and transgenic mice containing conditional *Tsc1*^{null} pyramidal neurons and astrocytes in the forebrain generating a global malformation associated with seizures[29; 30]. We found that in both models, there was a significant increase in vessel density associated with an increased total vessel length and decreased lacunarity. These data suggest that mTOR-dependent MCDs are hyperperfused independently of seizure activity and that dysmorphic neurons in the MCD are closer to blood vessels and have a greater access to nutrients. With respect to the rapamycin sensitivity, we found that a rapamycin treatment paradigm that attenuated neuronal alterations in the focal MCD model also

partially rescued vessel alterations in this model, but it did not prevent alterations in the global MCD model. These findings suggest that the dosage of rapamycin will need to be calibrated to the sizes of the MCD and the degree of mTOR activation to fully rescue vessel alterations.

Methods

Mice

All procedures and protocols were approved by Yale University Institutional Animal Care and Use Committee. All mice used were timed pregnant CD-1 mice (Charles River Laboratories) and pups that were born from those mothers. We also used transgenic mice generated by breeding R*Tsc1*$^{fl/fl}$ mice (fl: floxed and R: Rosa26R-Stop-tdTomato) with R*Tsc1*$^{wt/mut}$ (wt: wildtype and mut for mutant) that had been crossed with *Emx1*^{Cre} mice (see Figure 1A for diagram). The *Tsc1*$^{fl/fl}$ and *Tsc1*$^{wt/mut}$ mouse lines were generated by David J. Kwiatkowski (Brigham and Women's Hospital, Harvard Medical School, Cambridge, Massachusetts, USA) and were obtained from Jackson Labs and national cancer institute, respectively. The *Emx1*^{Cre} and R26R-tdTomato reporter mouse lines were obtained from Jackson Labs. Both male and female mice were used for analysis. Tail or toe samples were taken and were subjected to DNA isolation and PCR amplification. Amplicons were separated by standard electrophoresis methods. For genotyping transgenic mice, we used the previously reported primers[30; 31].

In utero electroporation and plasmids

Timed pregnant embryonic (E) 15 CD-1 mice were anesthetized and the uterine horns were exposed. DNA plasmid constructs were injected into the lateral ventricle of the fetuses (concentrations ranged from 1-2 μg/μl per construct depending on the experiment). Fast green was added at 0.01% w/v for visualization of injection. To electroporate constructs into neural progenitors, 5 mm tweezertrodes (BTX) were used to pass five 50 ms 39 V pulses. Plasmids included: pCAG-tdTomato[32], pCAG-TagBFP (gift from J. Breunig (Cedars Sinai, Los Angeles), pCAGGS-Rheb^{CA} (1.5 μg/μl, mutation S16H, gift from T. Maehama and K. Hanada, National Institute of Infectious Diseases, Tokyo, Japan[33]).

Transcardial perfusion and immunofluorescence

Mice were transcardially perfused with 100 μl Alexa Fluor 488-conjugated dextran (0.5%, 3,000 and 20,000 MW, Thermofisher, #D22910) for 3 minutes. Brains were then collected, fixed in 4% paraformaldehyde for 24 hours, and sectioned coronally on a vibratome (Leica VTS 1000) at a thickness of 100 μm. For immunofluorescence, free-floating sections were incubated for 1 hour in a blocking solution (2% bovine serum albumin and 0.1% Triton-X in PBS) at room temperature and then incubated with primary antibodies overnight at 4°C. Sections were washed with PBS + 0.05% Tween 20 and then placed in blocking solution containing secondary antibodies for 1 hour at room temperature. The primary antibodies used were rabbit anti-Cux1 (Santa Cruz sc-13024, 1:100) and rabbit anti-glial fibrillary acidic protein (GFAP) (CST, #12389, 1:1000), and the secondary antibody was a goat anti-rabbit Alexa Fluor 633 (ThermoFisher, #A-21070) used at 1:1000. All images were taken

using an FV1000 confocal microscope (Olympus). Data obtained with both dextran dyes were similar and were thus pooled.

Drug treatment

For in vivo injections, rapamycin (A.G. Scientific Inc., #R-1018) was dissolved in DMSO at a concentration of 12.5 mg/ml and resuspended in vehicle (0.25% PEG-400 and 0.25% Tween 80) at a final concentration of 0.1 mg/ml. Mice received 7 intraperitoneal injections of 0.5 mg/kg rapamycin every other day from P1 to P14. Vehicle treatment contained the same volume of DMSO.

Quantification of neuronal distribution, soma size, dendritic morphology, and vessel analysis

The number of tdTomato+ cells was counted using the Cell Counter plugin for ImageJ. Only cells within the grey matter of the cortex were quantified. For quantification of cells in layer 2-4, the boundary between layer 2-4 and layer 5 was determined using Cux1 staining. Soma size was quantified by outlining the soma of tdTomato+ cells and measuring the area using ImageJ. For the dendritic analyses, we performed Sholl analysis using Fuji simple neurite tracer as described before[30; 34] Vessels were analyzed in layer 2/3 in $Rheb^{CA}$-expressing mice and in all layers in transgenic *Tsc1* mice using automatic software AngioTool[35].

Analyses were performed in a blinded fashion. More specifically, after imaging brain sections, all images are saved using the same color and the file names are randomized. The condition is thus unknown to the investigator performing analysis.

Statistics

Data were analyzed and presented using Prism 7 (Graphpad). Statistical significance was determined using unpaired two-tail t-tests and one-way ANOVA with Tukey post-test. All errors bars are given as SEM.

Results

Transgenic *Tsc1* mice with global MCD display hypervascularization

To assess vessel density in global mTOR-dependent MCD, we used transgenic mice in which *Tsc1* was removed from forebrain pyramidal neurons and some astrocytes resulting in convulsive seizures and death at postnatal day (P) 18-21[29; 36]. To generate these mice, we bred R*Tsc1*$^{fl/fl}$ mice (fl: floxed and R: Rosa26R-Stop-tdTomato) with R*Tsc1*$^{wt/mut}$ (wt: wildtype and mut for mutant) that had been crossed with *Emx1*^{Cre} mice. This breeding scheme generated littermate *Emx1*^{Cre}-R*Tsc1*$^{fl/wt}$ and *Emx1*^{Cre}-R*Tsc1*$^{fl/mut}$ pups, corresponding to *Tsc1*^{het} mice containing tdTomato-positive *Tsc1*^{het} and *Tsc1*^{null} pyramidal neurons and some astrocytes in the forebrain, respectively (Fig. 1A), which recapitulated the genotypes of TSC patients[37]. Indeed, EMX1 is expressed by embryonic day (E) 9.5 in a subpopulation of dorsal telencephalic radial glia that generate pyramidal neurons and astrocytes in the forebrain[38]. As previously reported, transgenic *Tsc1* mice containing *Tsc1*^{null} cells displayed enlarged cortices compared to those containing *Tsc1*^{het} cells[29; 30; 36] (Fig. 1B and 1C). To label blood vessels, mice were transcardially perfused with a green

fluorescent dextran (Alexa Fluor 488, noted Dextran-AF488) dye at P14. In coronal sections at the level of the somatosensory cortex, an increased in vessel density was visible by eye in *Emx1*^{Cre}-R*Tsc1*$^{fl/mut}$ mice (Fig. 1C). To then analyze several parameters of vessel branching, we used the automatic software AngioTool[35]. In this software, a vessel is defined as a segment between two branching points or a branching point and an end-point. Figure 1D illustrates images of blood vessel modeling after analysis. Using this software, we found that vessel density, which is the percentage of area covered by vessels, significantly increased by ~25% (Figure 1E, statistics and N are in the figures). This change was accompanied by a 25% increase in junction density (branching index, Fig. 1F) and an 83% increase in total vessel length (normalized to the area, Fig. 1G). Consistent with the hypervascularization, there was a significant 34% decrease in the tissue lacunarity (Fig. 1H), which indicates that the "holes" formed by vessels became smaller and thus individual neurons are closer to blood vessels.

Mice with focal MCD display hypervascularization

Using transgenic *Tsc1* mice leads to a global forebrain MCD which is not representative of most patients' FCD that are more spatially restricted. In addition, using the transgenic *Tsc1* mice with global cortical malformation leads to seizure activity preventing us to assess whether the presence of dysmorphic neurons alone without seizure is sufficient to induce hypervascularization. We thus used our previously described model of a focal MCD, in which we manipulated mTOR activity in a subset of cortical neural progenitors during corticogenesis[28; 34]. In this model, a focal MCD in the somatosensory cortex did not lead to seizures while a focal MCD in the medial prefrontal cortex led to seizures that were visible starting at P21[28]. To generate this model, we introduced a plasmid expressing a constitutively active form of Rheb (Rheb^{CA} 1.5 μg/μl at E15)[28; 34; 39; 40], the canonical activator of mTOR, into neural progenitors lining the lateral ventricles of the developing cortex through *in utero* electroporation (IUE) (Fig. 2A). We introduced a concentration of Rheb^{CA} that does not lead to seizures following IUE in the medial prefrontal cortex[41]. For control, littermates were electroporated with a blue fluorescent protein (BFP) expressing plasmid. In both conditions, a red fluorescent protein (-tdTomato-)-expressing reporter was co-electroporated to visualize the targeted cells. Dextran-AF488 was transcardially perfused to label blood vessels at postnatal day (P) 14 (Fig. 2B). IUE performed at E15 consistently resulted in plasmid expression in the superficial layers (2/3) neurons of the targeted cortical area, the somatosensory cortex (Fig. 2C). By eye, we could readily observe that Rheb^{CA}-expressing neurons were misplaced and scattered across the cortical layers and their soma appeared larger (Fig. 2D). To further confirmed the lack of seizures, we immunostained for the astrocytic marker GFAP because astrocyte reactivity detected by increased GFAP staining accompanies seizure activity[28]. There was no increase in GFAP immunostaining (Supplementary Figure 1). As observed using transgenic mice, analysis using AngioTool in sections from P14 mice (Fig. 2E) revealed a significant 20% increase in vessel density (from 35% to 43% of covered area, Fig. 2F) associated with significant increases in their branching index (25%, Fig. 2G) and total vessel length (79%, Fig. 2H), and a significant 35% decrease in tissue lacunarity (Fig. 2I). Finally, the density of endpoints (i.e., open ended segments) was not altered (data not shown). To determine whether these vessel abnormalities extended outside the MCD, we analyzed non-electroporated regions surrounding the MCD or region

electroporated with BFP (Fig. 3A). There was no hypervascularization surrounding the MCD (Fig. 3B and C). These data further support the notion that hypervascularization occurred independently of seizures.

Decreasing mTOR activity with a non-saturating dose of rapamycin reduces hypervascularization in the focal but not the global MCD

Based on our past experience with rapamycin treatment in the focal MCD model, a 1 mg/kg dose of rapamycin every other day from P1 to the time of analysis normalized cell misplacement and dysmorphogenesis[28]. However, such a rapamycin dose severely altered mouse growth. Here, we aimed at testing a dose that would have a lesser impact on the mouse growth and would partially rescue the neuronal properties to remain in the linear range of rapamycin dose-effect. We thus tested rapamycin at 0.5 mg/kg as previously used[30] and assessed the efficacy of this rapamycin treatment on cell misplacement and dysmorphogenesis. As observed in Figure 2, $Rheb^{CA}$-expressing neurons did not reach layer 2/3 and were scattered across cortical layers (Fig. 4A). To quantify cell misplacement, we counted the number of cells that reached layer 2–4 identified by immunostaining for a marker of layer 2-4 neurons, Cux1. Only 48% of $Rheb^{CA}$ neurons reached their proper location (Fig. 4B). In addition, soma size and total dendritic length were significantly increased, which are typical alterations due to mTOR hyperactivity[42]. We then tested the effect of rapamycin on these alterations. A 14 day-long treatment of mice with a focal MCD partially rescued cell misplacement (Fig. 4A and B) and soma size (Fig. 4C and D), while it fully rescued total dendritic length (Fig. 4C and E). In transgenic *Tsc1* mice, the increased cortical thickness associated with a global cortical malformation (see Fig. 1C) was not rescued by rapamycin treatment (Fig. 5C).

We next assessed the efficacy of rapamycin treatment on blood vessels in each model. We found that rapamycin (at 0.5 mg/kg) partially prevented all the parameters of vascular abnormalities in the focal MCD, with rescues of vessel density and total vessel length, over-rescue for branching index (junction density) and partial rescue for lacunarity (Fig. 5A and B). Data were normalized to the control values used in Figure 1 and 2 because tissue processing and analyses were performed at the same time. By contrast, the same treatment in transgenic *Tsc1* mice did not rescue vessel alterations (Fig. 5C and D). We thus tested a higher dose of rapamycin (1 mg/kg) in transgenic *Tsc1* mice. This dose of rapamycin partially rescued all the vessel abnormalities (Fig. 5E and F). These data suggest that different types of malformations, meaning focal or global, with different activation of the mTOR signaling pathway display differential sensitivity to rapamycin treatment.

Discussion

Using mouse models of focal and global MCD, we found that both types of MCDs are associated with hypervascularization leading to abnormal vessel patterning and decreased lacunarity of the cortical tissue. In addition, hypervascularization was restricted to the focal MCD. As a correlate of this finding, dysmorphic neurons in the MCD are in closer proximity to blood-derived nutrients and metabolic supplies that may be permissive for sustaining intense firing. Our finding adds to the large body of literature with respect to

hyperperfusion of the epileptic foci and angiogenesis associated with epilepsy. It has been extensively reported that ictal activity is accompanied with hyperperfusion of the epileptic region. While it was thought that hyperperfusion resulted from functional alterations such as increased metabolism due to the epileptic activity, two recent studies in tissue from FCD and hemimegalencephaly patients provided evidence that hyperperfusion may also result from hypervascularization[18; 19] Our study further validates this finding in mice and confirms that hypervascularization occurs independently of seizures since P14 mice with FCD in the somatosensory cortex did not experience seizure activity[28]. Our model also characterized the types of vessel alterations, which include increased branching and total vessel length that are accompanied with decreased lacunarity. These changes likely lead to increased oxygenation and access to nutrients for cells in the MCD. Finally, we found that the vessel abnormalities were restricted to the focal MCD although small differences or a gradient of abnormalities may persist at the edge of the MCD.

Although we did not investigate how hypervascularization occurs in FCD or TSC, it has been shown that dysmorphic neurons expressing hyperactive mTOR during development release increased levels of VEGF[23-26], an angiogenic factor[43]. It is thus reasonable to think that VEGF released from dysmorphic neurons could contribute to the observed hypervascularization. During development, the big penetrating vessels are formed during embryonic life while capillarization of the brain parenchyma mostly occurs during postnatal life and is highly dynamic[44]. It is also known that neurogenesis and angiogenesis are coupled and altering one will affect the other[45; 46]. Thus, our data suggest that altered neurogenesis leads to alterations in vessel formation possibly through VEGF release. These data do not contradict with previous findings showing that epilepsy triggers angiogenesis[47]. It is likely that both phenomena, i.e., hypervascularization prior to seizures in the case of MCD and additional angiogenesis due to epileptic activity associated with MCDs, coexist. Another question relates to the outcome of altered vascularization on seizure activity. It is tempting to speculate that normalizing hypervascularization would metabolically starve neurons and limit their ability to sustain epileptiform activity. Consistent with such a prediction, it was reported that blocking angiogenesis prevented the establishment of clinical seizures in the pilocarpine rat model[47]. This prediction remains to be tested in our model perhaps using FCD generated in the medial prefrontal cortex because they are associated with seizures[28].

Finally, an important finding is that the blood vessel alterations in mice with a focal or a global MCD were quite similar, but only hypervascularization in the focal MCD was partially rescued by 0.5 mg/kg rapamycin treatment. The vessel abnormalities in the global MCD required higher dose of rapamycin (1 mg/kg) for a partial rescue. The discrepancy in rapamycin sensitivity between the two models showing similar hypervascularization remains unclear. The main differences between the two models include differences in the levels of mTOR hyperactivity, the size of the MCD and number of altered cells, and the occurrence or absence of seizures. It is possible that the vascular defect reached a maximum, and higher level of mTOR and/or seizure in the global MCD model requires more rapamycin to reach the threshold for a rescue. Importantly, these data suggest that patients with MCD of different sizes, which is common, or with different degrees of mTOR hyperactivity based on the genetic variants for *Tsc1* or *Tsc2* or mutations in the mTOR gene pathway will need

different doses of rapamycin for treating vessel alterations. There is a thus a strong need for personalized medicine in patients with mTOR-dependent MCD.

Supplementary Material

Refer to Web version on PubMed Central for supplementary material.

Acknowledgments:

This work was supported by NIH/NINDS R21 NS093510, DoD TS150058, and the Swebilius Foundation (AB). We thank Drs. K. Hanada and T. Maehama (National Institute of Infectious Diseases, Tokyo) for providing the Rheb^{CA} vector. We also thank Dr. Lena Nguyen for reading the present manuscript and provide comments.

References

1. Leventer RJ, Guerrini R, Dobyns WB. Malformations of cortical development and epilepsy. Dialogues Clin Neurosci 2008;10:47–62. [PubMed: 18472484]
2. Harvey AS, Cross JH, Shinnar S, et al. Defining the spectrum of international practice in pediatric epilepsy surgery patients. Epilepsia 2008;49:146–155. [PubMed: 18042232]
3. Blumcke I, Spreafico R, Haaker G, et al. Histopathological Findings in Brain Tissue Obtained during Epilepsy Surgery. N Engl J Med 2017;377:1648–1656. [PubMed: 29069555]
4. Baulac S, Ishida S, Marsan E, et al. Familial focal epilepsy with focal cortical dysplasia due to DEPDC5 mutations. Ann. Neurol 2015;77:675–683. [PubMed: 25623524]
5. Scheffer IE, Heron SE, Regan BM, et al. Mutations in mammalian target of rapamycin regulator DEPDC5 cause focal epilepsy with brain malformations. Ann Neurol 2014;75:782–787. [PubMed: 24585383]
6. Scerri T, Riseley JR, Gillies G, et al. Familial cortical dysplasia type IIA caused by a germline mutation in DEPDC5. Ann Clin Transl Neurol 2015;2:575–580. [PubMed: 26000329]
7. Leventer RJ, Scerri T, Marsh AP, et al. Hemispheric cortical dysplasia secondary to a mosaic somatic mutation in MTOR. Neurology 2015;84:2029–2032. [PubMed: 25878179]
8. Moller RS, Weckhuysen S, Chipaux M, et al. Germline and somatic mutations in the MTOR gene in focal cortical dysplasia and epilepsy. Neurol Genet 2016;2:e118. [PubMed: 27830187]
9. Jansen LA, Mirzaa GM, Ishak GE, et al. PI3K/AKT pathway mutations cause a spectrum of brain malformations from megalencephaly to focal cortical dysplasia. Brain 2015.
10. Nakashima M, Saitsu H, Takei N, et al. Somatic mutations in the MTOR gene cause focal cortical dysplasia type IIb. Ann. Neurol 2015.
11. Lim JS, Gopalappa R, Kim SH, et al. Somatic Mutations in TSC1 and TSC2 Cause Focal Cortical Dysplasia. Am J Hum Genet 2017;100:454–472. [PubMed: 28215400]
12. Lim JS, Kim WI, Kang HC, et al. Brain somatic mutations in MTOR cause focal cortical dysplasia type II leading to intractable epilepsy. Nat. Med 2015.
13. Hoelz H, Coppenrath E, Hoertnagel K, et al. Childhood-Onset Epileptic Encephalopathy Associated With Isolated Focal Cortical Dysplasia and a Novel TSC1 Germline Mutation. Clin EEG Neurosci 2018;49:187–191. [PubMed: 28762286]
14. Crino PB, Nathanson KL, Henske EP. The tuberous sclerosis complex. N. Engl. J. Med 2006;355:1345–1356. [PubMed: 17005952]
15. Blumcke I, Thom M, Aronica E, et al. The clinicopathologic spectrum of focal cortical dysplasias: a consensus classification proposed by an ad hoc Task Force of the ILAE Diagnostic Methods Commission. Epilepsia 2011;52:158–174. [PubMed: 21219302]
16. Aronica E, Becker AJ, Spreafico R. Malformations of cortical development. Brain Pathol 2012;22:380–401. [PubMed: 22497611]
17. Kim JH, Im KC, Kim JS, et al. Ictal hyperperfusion patterns in relation to ictal scalp EEG patterns in patients with unilateral hippocampal sclerosis: a SPECT study. Epilepsia 2007;48:270–277. [PubMed: 17295620]

18. Wintermark P, Lechpammer M, Warfield SK, et al. Perfusion Imaging of Focal Cortical Dysplasia Using Arterial Spin Labeling: Correlation With Histopathological Vascular Density. J Child Neurol 2013;28:1474–1482. [PubMed: 23696629]
19. Wintermark P, Roulet-Perez E, Maeder-Ingvar M, et al. Perfusion abnormalities in hemimegalencephaly. Neuropediatrics 2009;40:92–96. [PubMed: 19809940]
20. Koh S, Jayakar P, Dunoyer C, et al. Epilepsy surgery in children with tuberous sclerosis complex: presurgical evaluation and outcome. Epilepsia 2000;41:1206–1213. [PubMed: 10999561]
21. Matsuda K, Mihara T, Tottori T, et al. Neuroradiologic findings in focal cortical dysplasia: histologic correlation with surgically resected specimens. Epilepsia 2001;42 Suppl 6:29–36.
22. Epilepsy Duncan R., cerebral blood flow, and cerebral metabolic rate. Cerebrovasc Brain Metab Rev 1992;4:105–121. [PubMed: 1627438]
23. Parker WE, Orlova KA, Heuer GG, et al. Enhanced epidermal growth factor, hepatocyte growth factor, and vascular endothelial growth factor expression in tuberous sclerosis complex. Am. J. Pathol 2011;178:296–305. [PubMed: 21224066]
24. Feliciano DM, Zhang S, Quon JL, et al. Hypoxia-inducible factor 1a is a Tsc1-regulated survival factor in newborn neurons in tuberous sclerosis complex. Hum. Mol. Genet 2013;22:1725–1734. [PubMed: 23349360]
25. Boer K, Troost D, Spliet WG, et al. Cellular distribution of vascular endothelial growth factor A (VEGFA) and B (VEGFB) and VEGF receptors 1 and 2 in focal cortical dysplasia type IIB. Acta Neuropathol 2008;115:683–696. [PubMed: 18317782]
26. El-Hashemite N, Walker V, Zhang H, et al. Loss of Tsc1 or Tsc2 induces vascular endothelial growth factor production through mammalian target of rapamycin. Cancer Res 2003;63:5173–5177. [PubMed: 14500340]
27. French JA, Lawson JA, Yapici Z, et al. Adjunctive everolimus therapy for treatment-resistant focal-onset seizures associated with tuberous sclerosis (EXIST-3): a phase 3, randomised, double-blind, placebo-controlled study. Lancet 2016;388:2153–2163. [PubMed: 27613521]
28. Hsieh LS, Wen J, Claycomb K, et al. Convulsive seizures from experimental focal cortical dysplasia occur independently of cell misplacement. Nature Communications 2016:In Press.
29. Magri L, Cambiaghi M, Cominelli M, et al. Sustained activation of mTOR pathway in embryonic neural stem cells leads to development of tuberous sclerosis complex-associated lesions. Cell Stem Cell 2011;9:447–462. [PubMed: 22056141]
30. Zhang L, Bartley CM, Gong X, et al. MEK-ERK1/2-Dependent FLNA Overexpression Promotes Abnormal Dendritic Patterning in Tuberous Sclerosis Independent of mTOR. Neuron 2014;84:78–91. [PubMed: 25277454]
31. Feliciano DM, Su T, Lopez J, et al. Single-cell Tsc1 knockout during corticogenesis generates tuber-like lesions and reduces seizure threshold in mice. J. Clin. Invest 2011;121:1596–1607. [PubMed: 21403402]
32. Pathania M, Torres-Reveron J, Yan L, et al. miR-132 enhances dendritic morphogenesis, spine density, synaptic integration, and survival of newborn olfactory bulb neurons. PLoS. ONE 2012;7:e38174. [PubMed: 22693596]
33. Maehama T, Tanaka M, Nishina H, et al. RalA functions as an indispensable signal mediator for the nutrient-sensing system. J. Biol. Chem 2008;283:35053–35059. [PubMed: 18948269]
34. Lin TV, Hsieh L, Kimura T, et al. Normalizing translation through 4E-BP prevents mTOR-driven cortical mislamination and ameliorates aberrant neuron integration. Proc. Natl. Acad. Sci. U. S. A 2016;113:11330–11335. [PubMed: 27647922]
35. Zudaire E, Gambardella L, Kurcz C, et al. A computational tool for quantitative analysis of vascular networks. PLoS One 2011;6:e27385. [PubMed: 22110636]
36. Carson RP, Van Nielen DL, Winzenburger PA, et al. Neuronal and glia abnormalities in Tsc1-deficient forebrain and partial rescue by rapamycin. Neurobiol. Dis 2012;45:369–380. [PubMed: 21907282]
37. Tyburczy ME, Dies KA, Glass J, et al. Mosaic and Intronic Mutations in TSC1/TSC2 Explain the Majority of TSC Patients with No Mutation Identified by Conventional Testing. PLoS Genet 2015;11:e1005637. [PubMed: 26540169]

38. Gorski JA, Talley T, Qiu M, et al. Cortical excitatory neurons and glia, but not GABAergic neurons, are produced in the Emx1-expressing lineage. J. Neurosci 2002;22:6309–6314. [PubMed: 12151506]

39. Lafourcade CA, Lin TV, Feliciano DM, et al. Rheb activation in subventricular zone progenitors leads to heterotopia, ectopic neuronal differentiation, and rapamycin-sensitive olfactory micronodules and dendrite hypertrophy of newborn neurons. J. Neurosci 2013;33:2419–2431. [PubMed: 23392671]

40. Hartman NW, Lin TV, Zhang L, et al. mTORC1 Targets the Translational Repressor 4E-BP2, but Not S6 Kinase 1/2, to Regulate Neural Stem Cell Self-Renewal In Vivo. Cell Rep 2013;5:433–444. [PubMed: 24139800]

41. Nguyen LH, Mahadeo T, Bordey A. mTOR Hyperactivity Levels Influence the Severity of Epilepsy and Associated Neuropathology in an Experimental Model of Tuberous Sclerosis Complex and Focal Cortical Dysplasia. J Neurosci 2019.

42. Feliciano DM, Hartman NW, Lin TV, et al. A circuitry and biochemical basis for tuberous sclerosis symptoms: from epilepsy to neurocognitive deficits. Int. J. Dev. Neurosci 2013:667–678. [PubMed: 23485365]

43. Jin K, Zhu Y, Sun Y, et al. Vascular endothelial growth factor (VEGF) stimulates neurogenesis in vitro and in vivo. Proc. Natl. Acad. Sci. U. S. A 2002;99:11946–11950. [PubMed: 12181492]

44. Zeller K, Vogel J, Kuschinsky W. Postnatal distribution of Glut1 glucose transporter and relative capillary density in blood-brain barrier structures and circumventricular organs during development. Brain Res Dev Brain Res 1996;91:200–208 [PubMed: 8852370]

45. Palmer TD, Willhoite AR, Gage FH. Vascular niche for adult hippocampal neurogenesis. J. Comp Neurol 2000;425:479–494. [PubMed: 10975875]

46. Hallene KL, Oby E, Lee BJ, et al. Prenatal exposure to thalidomide, altered vasculogenesis, and CNS malformations. Neuroscience 2006;142:267–283. [PubMed: 16859833]

47. Benini R, Roth R, Khoja Z, et al. Does angiogenesis play a role in the establishment of mesial temporal lobe epilepsy? Int J Dev Neurosci 2016;49:31–36. [PubMed: 26773167]

Key bullet points

1. Hypervascularization accompanies mTOR-dependent MCD.
2. Hypervascularization precedes the occurrence of seizures.
3. Vessel abnormalities include increased vessel density, branching index, and total vessel length, and decreased tissue lacunarity.
4. Rapamycin differentially rescues vessel abnormalities in focal and global MCD.

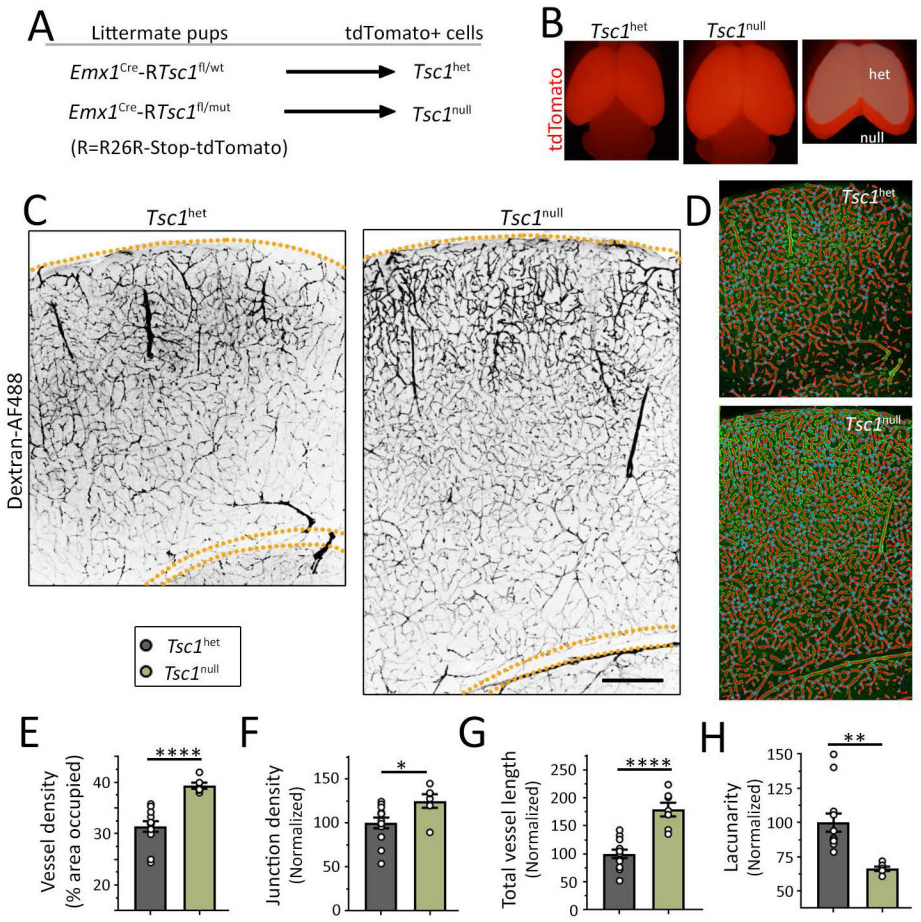

Figure 1: Transgenic *Tsc1* mice containing a global mTOR-dependent MCD display hypervascularization.

(A) Diagram of the transgenic *Tsc1* mice used (wt: wildtype, fl: floxed, and mut: mutant) that contained *Tsc1*^{het} cells or *Tsc1*^{null} cells in a heterozygote (het) brains. **(B)** Images of the brains of the two mouse genotypes. The forebrain is tdTomato-positive and is enlarged in mice containing *Tsc1*^{null} cells as further illustrated by overlapping both cortices (far right). **(C)** Images of Dextran-AF488-filled blood vessels in coronal sections containing *Tsc1*^{het} cells (left) and *Tsc1*^{null} cells (right) in the somatosensory cortex. Scale bars: 400 μm. **(D)** Examples of the modeling of blood vessels for analysis. **(E-H)** Bar graphs of the different vessel parameters, including vessel density (E), normalized junction density (F), total vessel length (G, normalized to control and by the area), and normalized lacunarity (H). N≥2 sections per 3-5 mice (datapoints= values per section). Student's t-test, ****: P<0.0001, **:P<0.01, *:P<0.05.

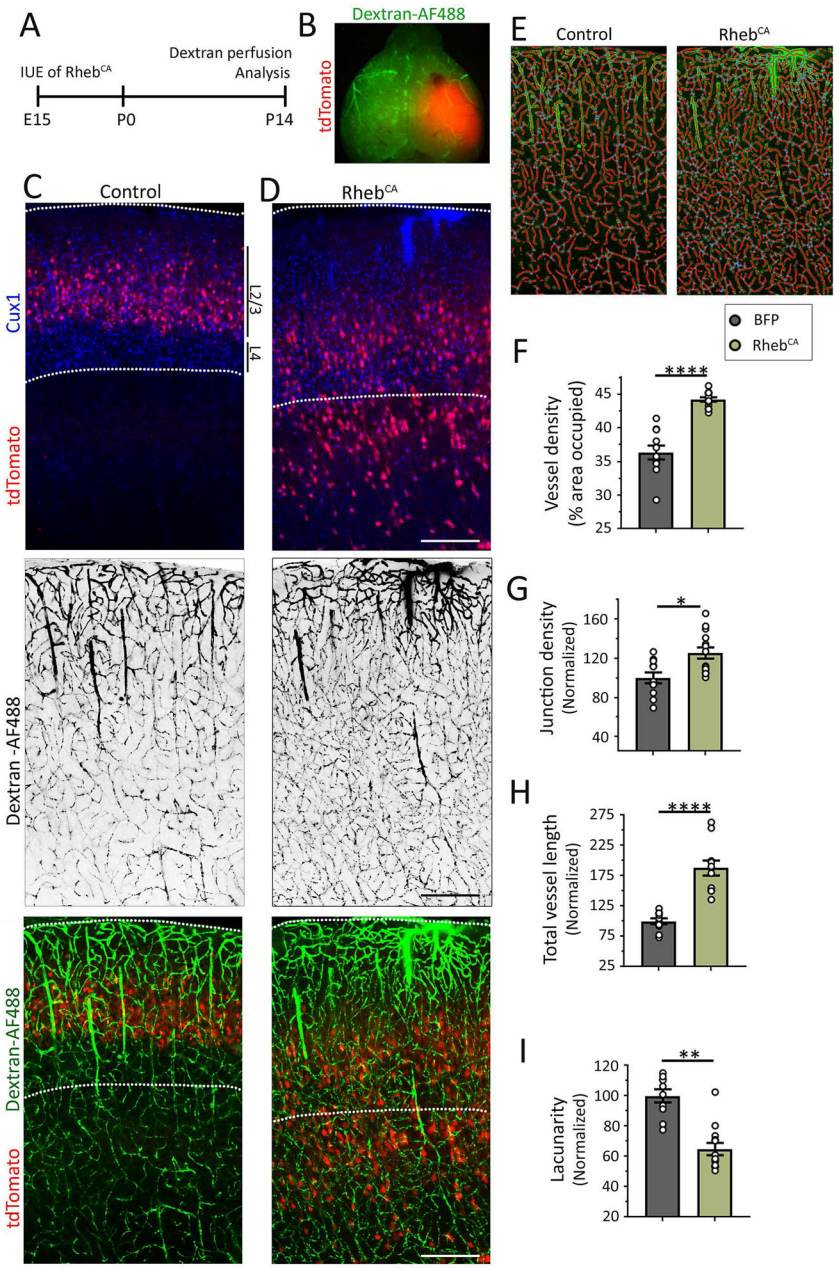

Figure 2: Focal MCD are associated with hypervascularization.

(A) Diagram of experimental design. **(B)** Image of the tdTomato-fluorescent MCD and dextran-AF488 fluorescence throughout the vessels. **(C and D)** Images of tdTomato-positive cells containing BFP (panels in C, BFP not shown) or Rheb^{CA} (panels in D) and Cux1 immunostaining (pseudo-colored blue), and images of dextran-AF488-filled blood vessels in black (middle panels) and in green superimposed with tdTomato-positive neurons (bottom panels) in coronal sections from the somatosensory cortex. Scale bars: 300 μm. **(E)** Examples of the modeling of blood vessels for analysis. **(F-I)** Bar graphs of vessel density (F), normalized junction density (G), normalized total vessel length (normalized to control and the area, H), and normalized lacunarity (I) in control (grey) and Rheb^{CA} (green)

condition. N≥2 sections per mouse from 4-5 mice (datapoints= value per section). Student's t-test, ****: P<0.0001, **:P<0.01, *:P<0.05.

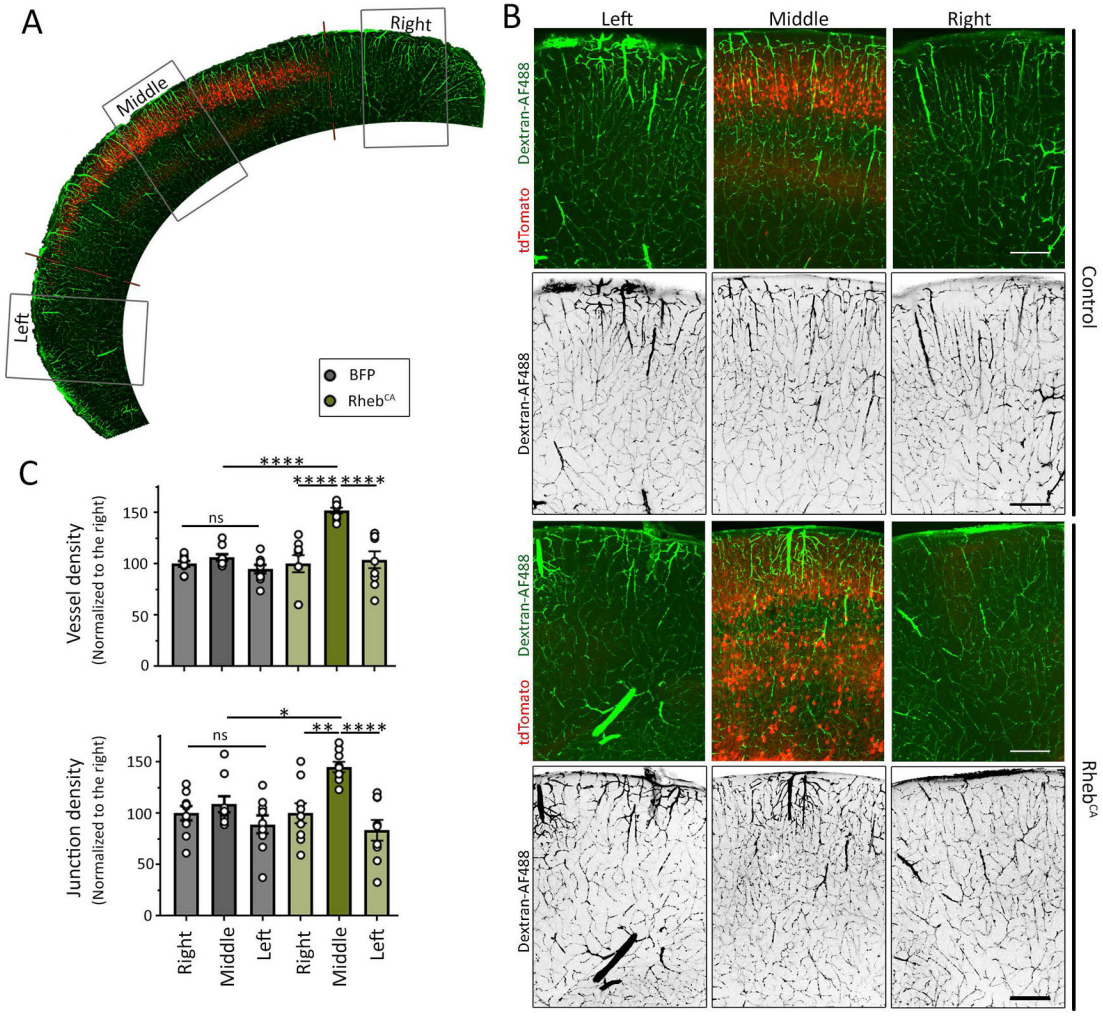

Figure 3: Hypervascularization is restricted to the MCD.

(A) Low magnification image of the cortex containing the tdTomato-fluorescent electroporated region and dextran-AF488 fluorescence vessels. **(B)** Images of tdTomato-positive cells containing a control plasmid (noted control) or Rheb^{CA} (noted in the right) and dextran-AF488-filled blood vessels in green or in black (shown alone) in coronal sections from the somatosensory cortex. Scale bars: 200 μm. **(C)** Bar graphs of vessel density and normalized junction density in control (grey) and Rheb^{CA} (green) conditions. N≥2 sections per mouse from 4-5 mice (datapoints on graph= value per section). Two-way ANOVA followed by Tukey test, ****: P<0.0001, **:P<0.01, *:P<0.05, and ns: not significant.

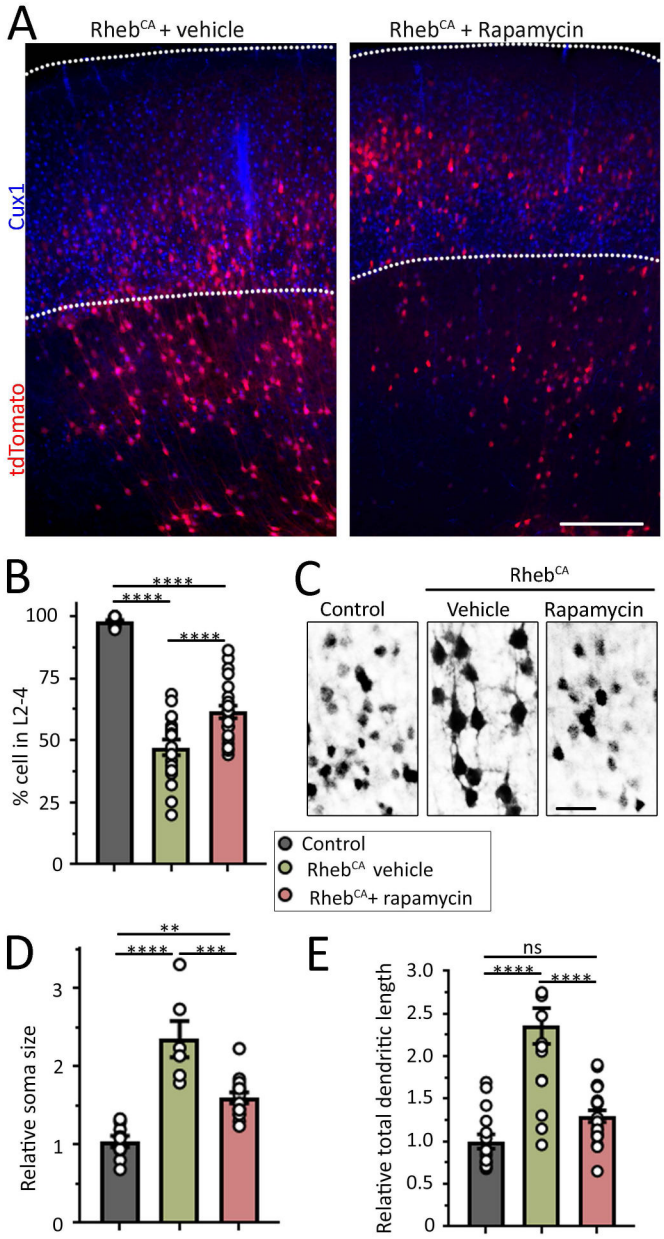

Figure 4: Rapamycin partially rescues neuronal defects in focal MCDs. (A Figure 4: Rapamycin partially rescues neuronal defects in focal MCDs.

(A) Images of tdTomato-positive Rheb^{CA}-expressing neurons and Cux1 immunostaining in coronal sections from mice electroporated with Rheb^{CA} at E15 and repeated with either vehicle or 0.5 mg/kg rapamycin from P1 to P14 every other day. A section containing control BFP-electroporated neurons is shown in Figure 2. Scale bars: 300 μm. **(B)** Bar graphs of the percentage (%) of tdTomato+ control neurons (grey) and Rheb^{CA}-expressing neurons in L2-4 (based on Cux1 staining) in mice treated with vehicle (green) or rapamycin (red). **(C)** Images of control neurons in mice electroporated with BFP + tdTomato and Rheb^{CA}-expressing neurons in mice electroporated with Rheb^{CA} + tdTomato and treated with vehicle or rapamycin. **(D and E)** Bar graphs of the soma size and total dendritic length

of control neurons (grey) and $Rheb^{CA}$ neurons in mice treated with vehicle (green) or rapamycin (red). N>3 mice, 2 sections per mouse (each datapoint is the mean from >8 neurons per section for dendrite analysis and >12 neurons for cell size per section). One-way ANOVA with Tukey post-test. ****: P<0.0001, **:P<0.01, *:<P0.05, ns: not significant.

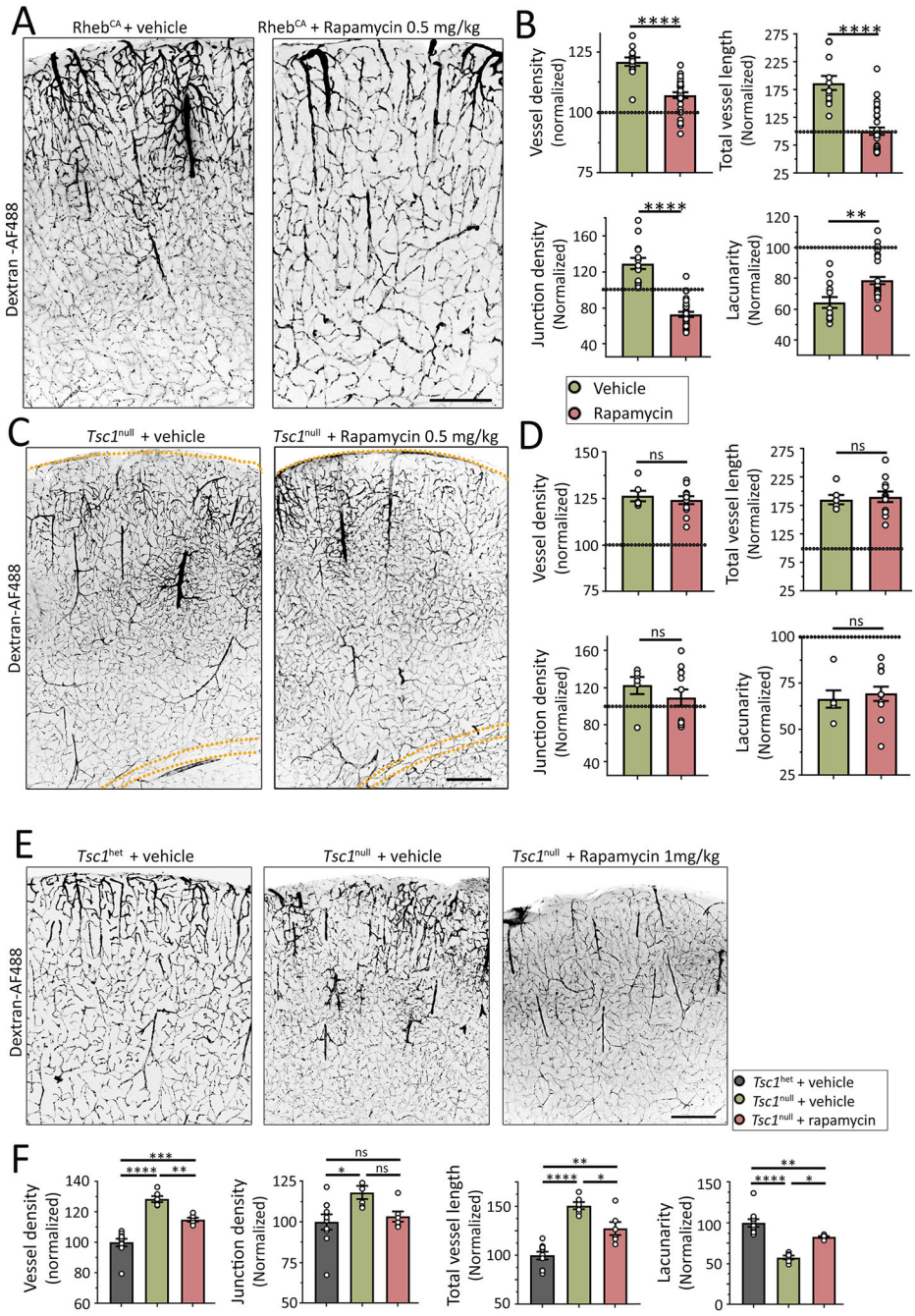

Figure 5: Rapamycin differentially reduces hypervascularization in focal and global MCDs.

(A and C) Images of Dextran-AF488-filled blood vessels in coronal sections containing Rheb^{CA} neurons (A) or *Tsc1*^{null} cells (C) in the somatosensory cortex of mice treated with vehicle (left) or 0.5 mg/kg rapamycin (right). Mice with Rheb^{CA} neurons had a focal MCD and transgenic mice with *Tsc1*^{null} cells had a global MCD. Scale bars: 300 μm (A) and 500 μm (C). **(B and D)** Bar graphs of the different vessel parameters in both sets of mice with focal (B) or global MCD (D). Values were normalized to their respective control shown in Figure 1 and 2. **(E)** Images of Dextran-AF488-filled blood vessels in coronal sections

containing *Tsc1*^{het} or *Tsc1*^{null} cells in the somatosensory cortex of mice treated with vehicle (left) or 1 mg/kg rapamycin. Scale bar: 200 μm. **(F)** Bar graphs of the different vessel parameters in mice with global MCD. N≥2 sections from 3-5 mice. Student's t-test in B and D or one-way ANOVA in F, ****: p<0.0001, **:P<0.01, *:P<0.05, and ns: not significant.